

Supporting Information

Integration of mesoporous nickel cobalt oxides nanosheets with ultrathin layer carbon wrapped TiO₂ nanotube arrays for high-performance supercapacitors

Cuiping Yu^a, Yan Wang^{*abc}, Jianfang Zhang^a, Xia Shu^{ac}, Jiewu Cui^{ac}, Yongqiang Qin^{ac}, Hongmei Zheng^{ac}, Jiaqin Liu^{ac}, Yong Zhang^{ac}, Yucheng Wu^{*ac}

a. School of Materials Science and Engineering, Hefei University of Technology, Hefei 230009, P. R. China.

b. Department of Material Science and NanoEngineering, Rice University, Houston, Texas 77005, United States.

c. Key Laboratory of Advanced Functional Materials and Devices of Anhui Province, Hefei 230009, P. R. China.

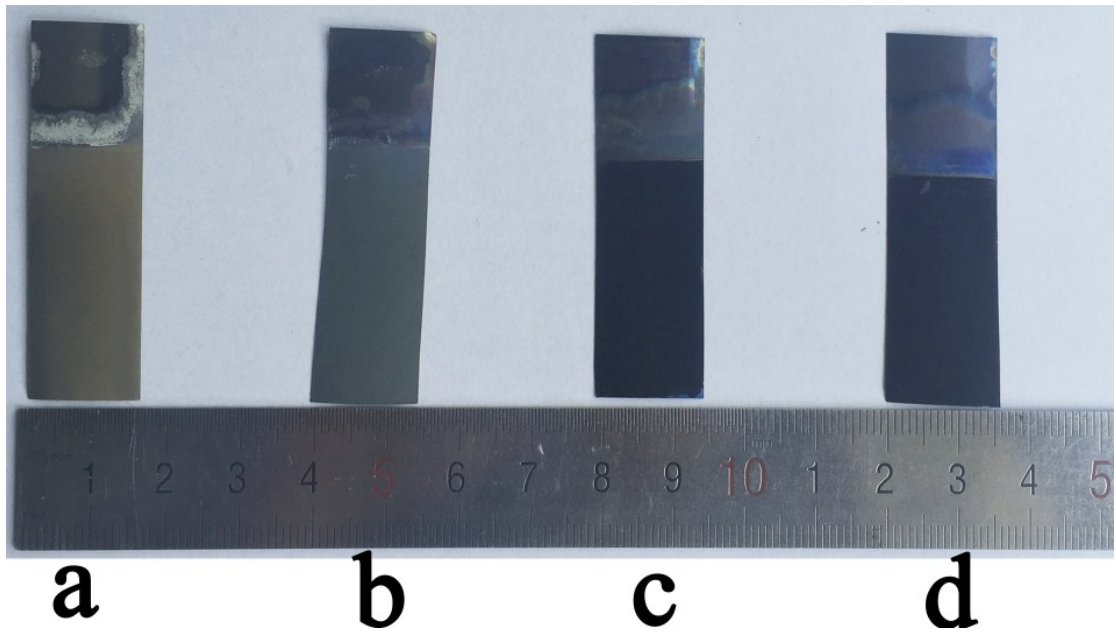


Fig. S1 Optical photos of a) anodized TNAs; b) TNAs; c) C-TNAs and d) nickel cobalt oxides/C-TNAs.

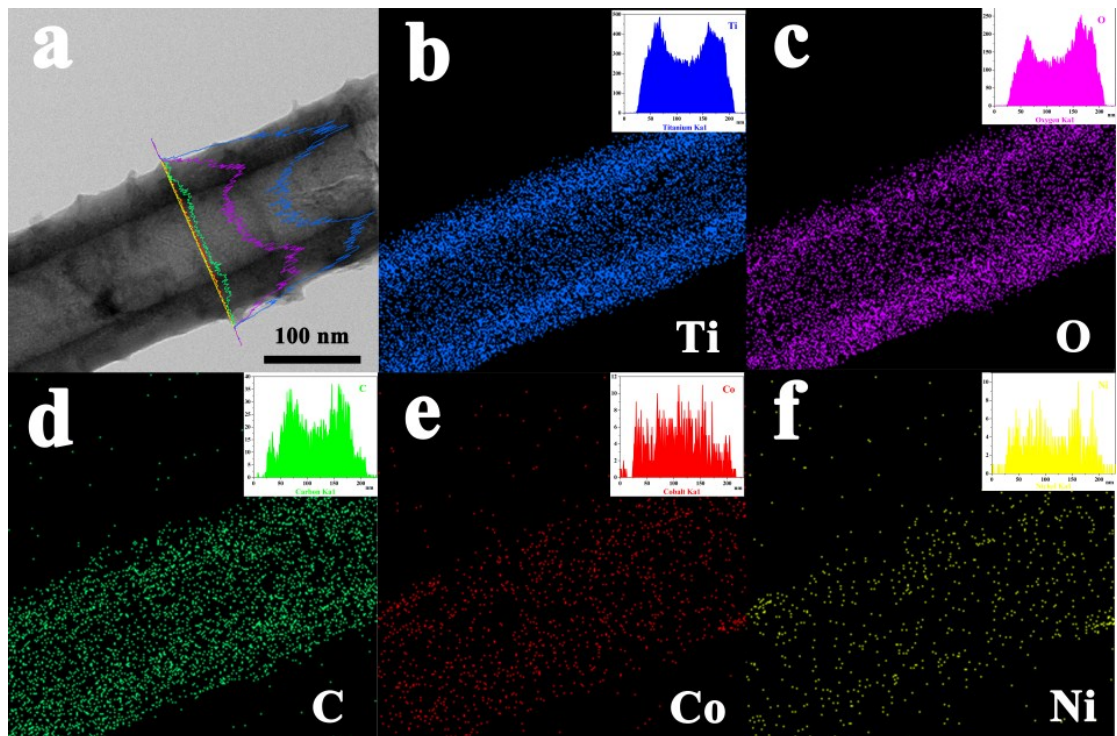


Fig. S2 a) TEM image of precursor decorated C-TNAs; EDS elemental mapping of b) Ti; c) O; d) C; e) Co and f) Ni. The inset show the corresponding EDS elemental distribution.

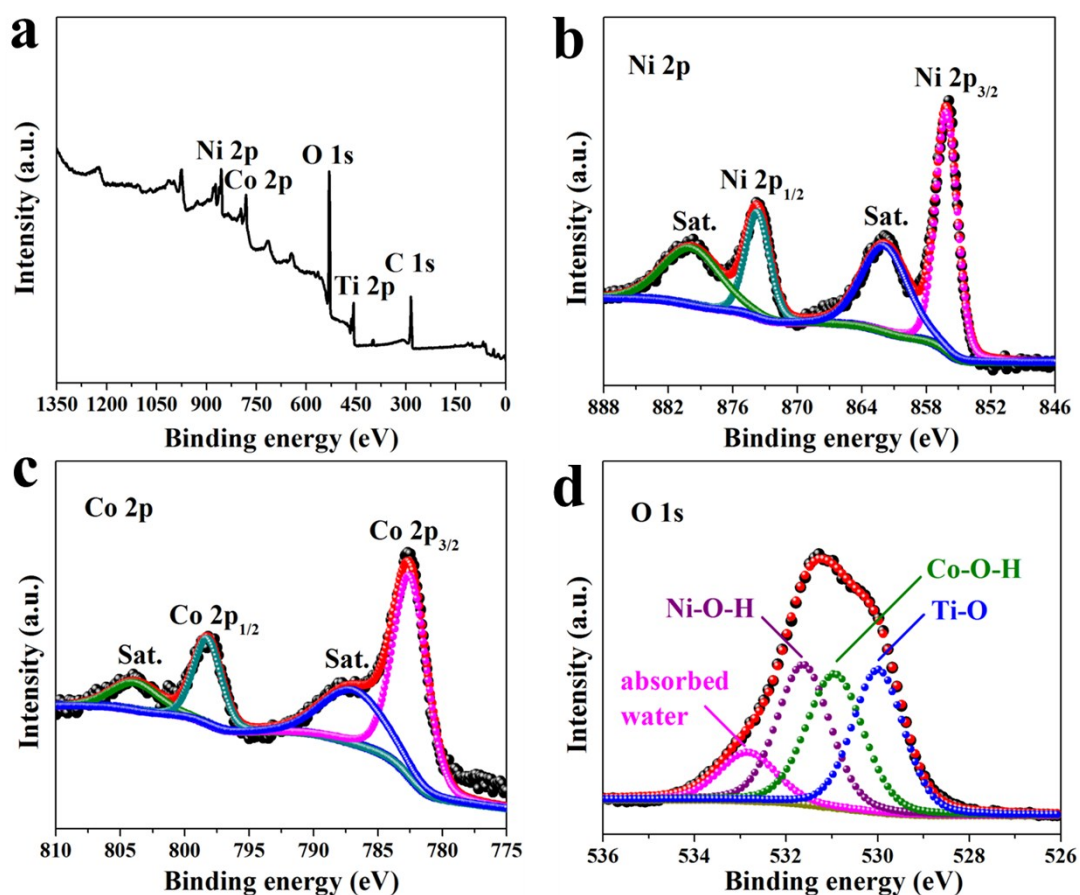


Fig. S3 a) XPS survey spectrum and b) Ni 2p; c) Co 2p; d) O 1s spectra of precursor of Ni-Co-3:3/C-TNAs.

The XPS survey spectrum clearly shows the presence of Ni, Co, Ti, O and C in the composite (Fig. S3a). The high-resolution XPS spectrum of Ni 2p (Fig. S3b) indicates that the two peaks located at 873.7 eV and 856.1 eV are ascribed to Ni 2p_{1/2} and Ni 2p_{3/2}, indicating the Ni²⁺ in nickel cobalt hydroxides.^[1] Similarly, in Fig. S3c, the peaks at 798.2 eV and 782.5 eV correspond to Co²⁺ in nickel cobalt hydroxides.^[2] In addition, the O 1s spectra (Fig. S3d) can be divided into four main peaks, Ni-O-H (531.9 eV), Co-O-H (531 eV), Ti-O (529.9 eV) and absorbed water (532.9 eV). In summary, the XPS spectra of precursor of Ni-Co-3:3/C-TNAs can prove that the precursor correspond to nickel cobalt hydroxides.

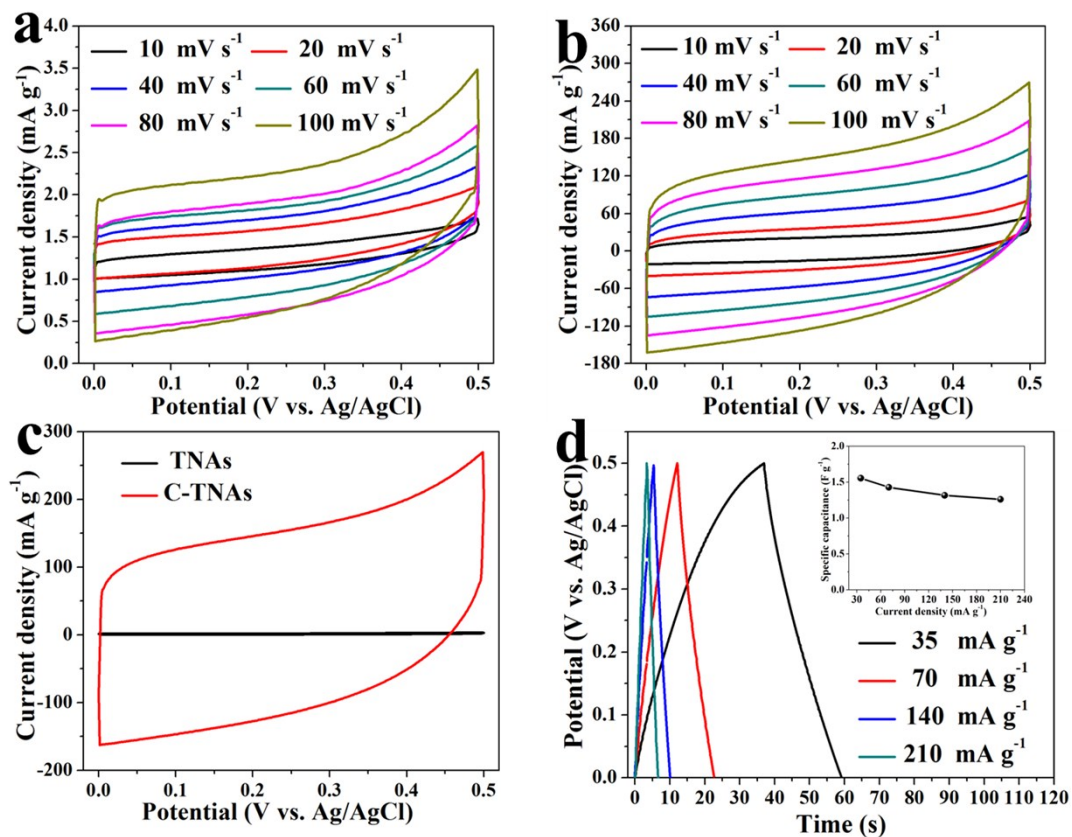


Fig. S4 CV curves of a) TNAs and b) C-TNAs; c) CV curves of TNAs and C-TNAs at a scan rate of 100 mV s^{-1} , d) GCD curves of C-TNAs at different current densities (inset shows the specific capacitance at different current densities).

In Fig. S4c, according to Equation 1 in the main paper, the specific capacitance from CV curve of C-TNAs (1.33 F g^{-1}) is 83 times higher than that of TNAs (16.02 mF g^{-1}).

The specific capacitance of C-TNAs in the GCD curves can be calculated using Equation 2 and the result is presented in the inset of Figure S4d, and specific capacitance of C-TNAs can reach 1.55 F g^{-1} at current density of 35 mA g^{-1} .

Table S1 Relative BET surface area of TNAs, C-TNAs and nickel cobalt oxides decorated C-TNAs samples attached to Ti foil

Sample	Relative BET specific surface area ($\text{m}^2 \text{cm}^{-2}$)
TNAs	0.0951
C-TNAs	0.1187
Ni-Co-1:5/C-TNAs	0.1613
Ni-Co-2:4/C-TNAs	0.1841
Ni-Co-3:3/C-TNAs	0.1980
Ni-Co-4:2/C-TNAs	0.1651

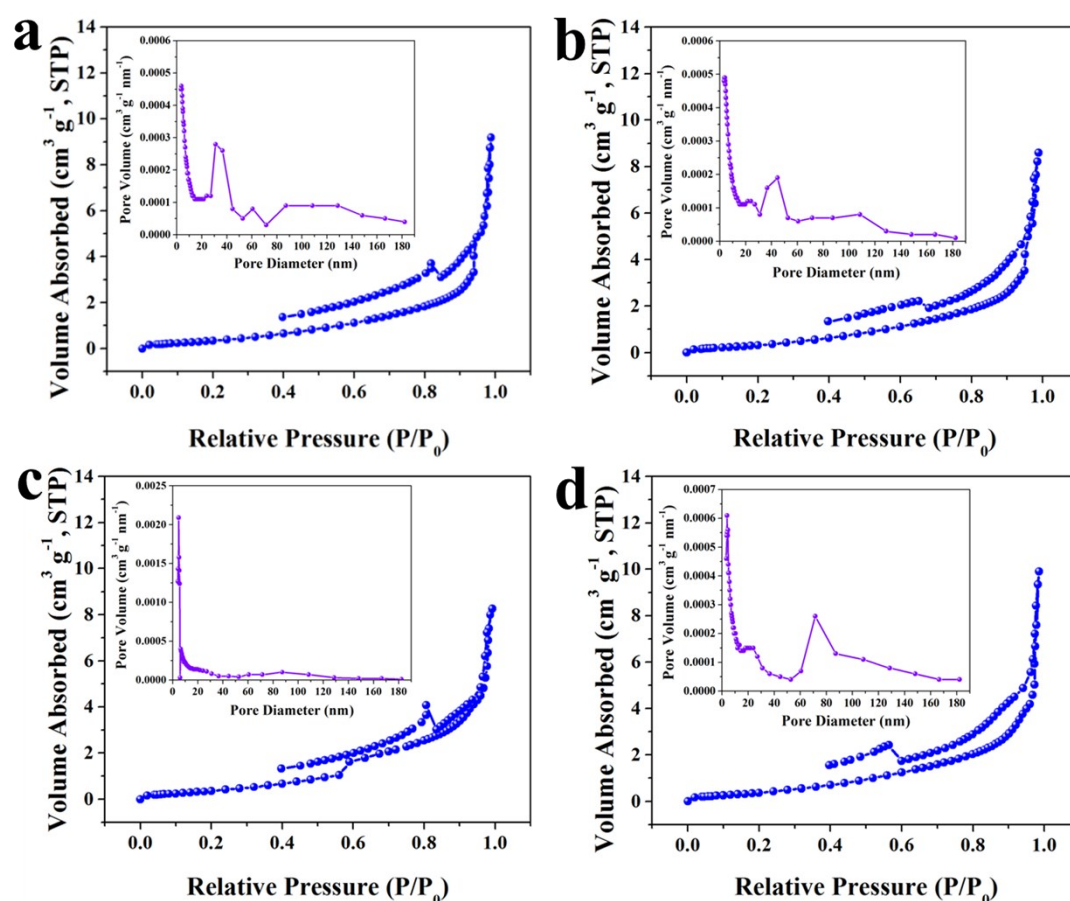


Fig. S5 N_2 adsorption and desorption isotherms of a) Ni-Co-1:5/C-TNAs, b) Ni-Co-2:4/C-TNAs, c) Ni-Co-3:3/C-TNAs and d) Ni-Co-4:2/C-TNAs. (insert shows the corresponding pore size distributions).

Table S2 Percentage of pores with different

diameter in four nickel cobalt oxides decorated C-TNAs

Pore diameter range (nm)	Percentage (%)			
	Ni-Co-1:5 /C-TNAs	Ni-Co-2:4 /C-TNAs	Ni-Co-3:3 /C-TNAs	Ni-Co-4:2 /C-TNAs
Under 6	6.80	8.98	18.58	7.08
6-8	2.84	3.80	4.83	2.84
8-10	2.03	2.75	3.33	2.11
10-12	1.90	2.50	3.17	2.07
12-16	2.40	3.16	4.04	2.80
16-20	2.80	3.51	4.51	3.37
20-80	34.93	42.47	27.00	34.19
over 80	46.29	32.83	34.53	45.55

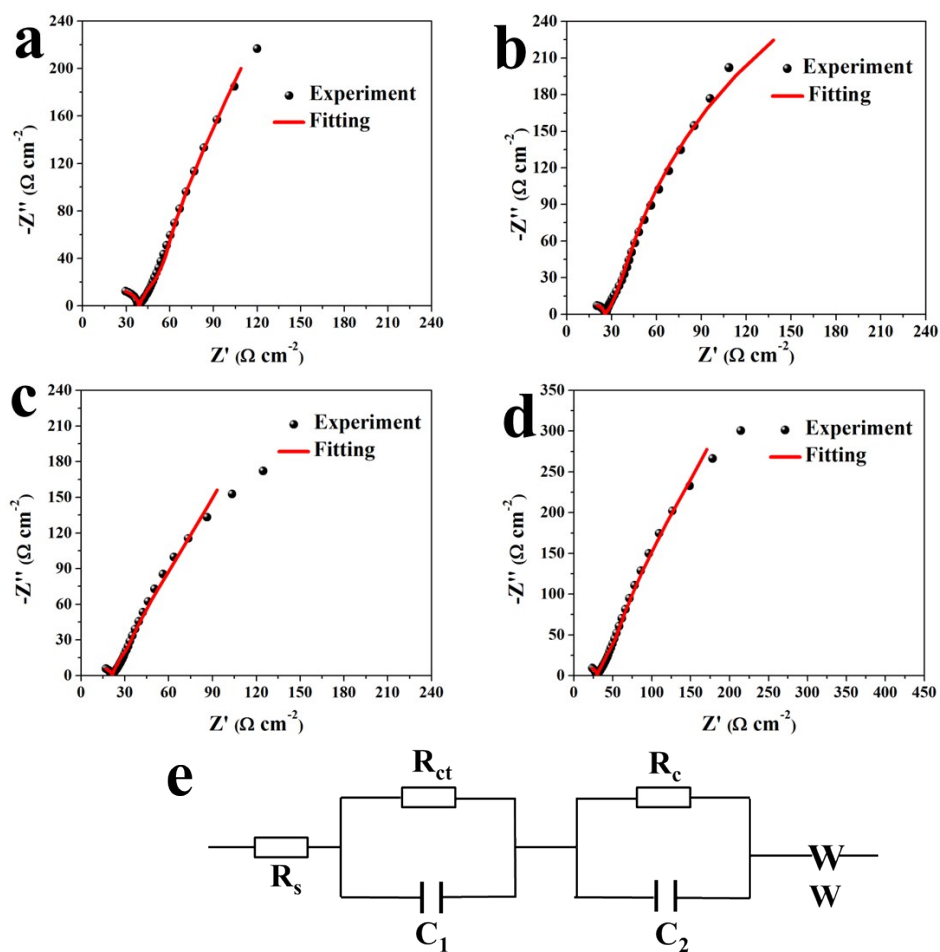


Fig. S6 Fitting curves of a) Ni-Co-1:5/C-TNAs; b) Ni-Co-2:4/C-TNAs; c) Ni-Co-3:3/C-TNAs; d) Ni-Co-4:2/C-TNAs and e) equivalent circuit.

Table S3 Fitting results of EIS curves

Sample	R_s ($\Omega \text{ cm}^{-2}$)	R_{ct} ($\Omega \text{ cm}^{-2}$)	R_c ($\Omega \text{ cm}^{-2}$)
Ni-Co-1:5/C-TNAs	11.74	26.12	823.5
Ni-Co-2:4/C-TNAs	9.60	15.66	540.5
Ni-Co-3:3/C-TNAs	7.53	12.95	337.2
Ni-Co-4:2/C-TNAs	7.68	20.97	565.7

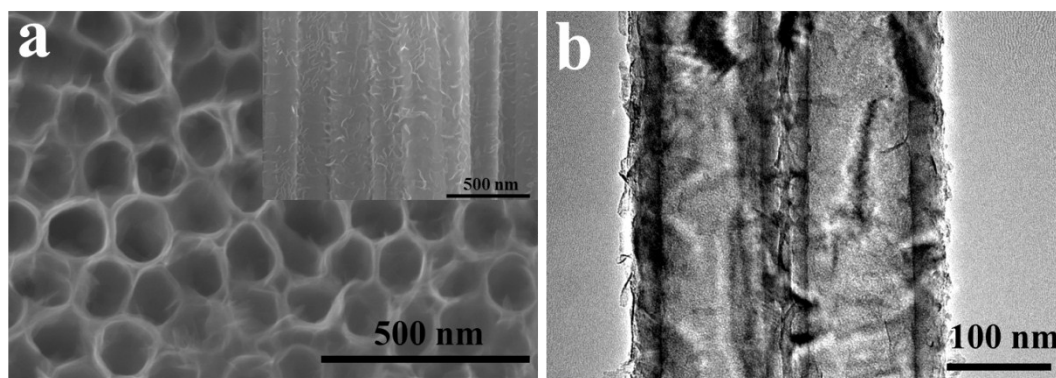


Fig. S7 a) FESEM image and b) TEM image of Ni-Co-3:3/C-TNAs after cycling for 5000 cycles.

Synthesis of nickel oxide/C-TNAs (or cobalt oxide/C-TNAs)

0.3 mmol $\text{Ni}(\text{NO}_3)_2 \cdot 6\text{H}_2\text{O}$ (or $\text{Co}(\text{NO}_3)_2 \cdot 6\text{H}_2\text{O}$) was dissolved in 50ml Milli-Q water, and then 1.5 mmol urea ($\text{CO}(\text{NH}_2)_2$) was added into the above aqueous solution. After ultrasonic treatment for 20 min, homogeneous precursor aqueous solution was obtained, and the precursor solution was transferred into 100 ml deposition instruments. And then C-TNAs were placed into the deposition instrument. Subsequently, the deposition instrument was kept in a chemical bath at 80°C for 10 h. After cooling down to room temperature naturally, C-TNAs with loaded precursors were taken out from reaction media, washed with Milli-Q water and ethanol several times to remove the impurities, and then dried at 60 °C overnight. The formed precursor was heated from room temperature to 350 °C with a heating rate of 1 °C min⁻¹ and maintained at 350 °C for 2 h to obtain the desired nickel oxide/C-TNAs (or cobalt oxide/C-TNAs).

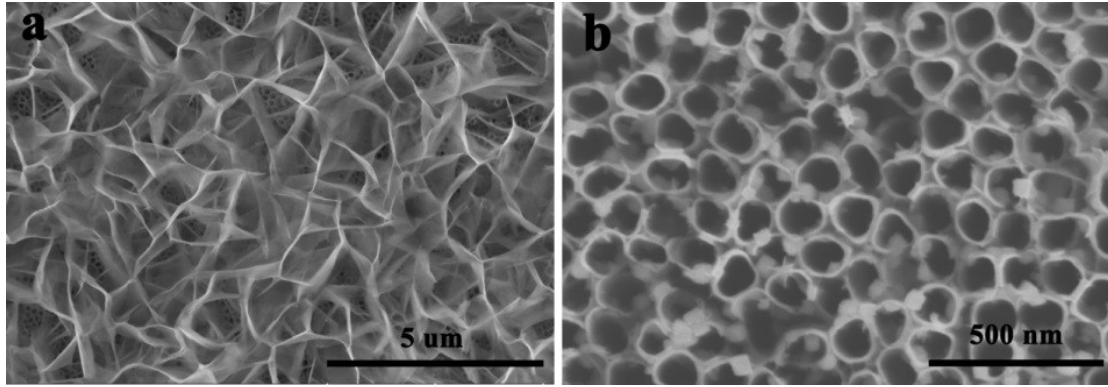


Fig. S8 FESEM images of a) nickel oxide/C-TNAs; b) cobalt oxide/C-TNAs.

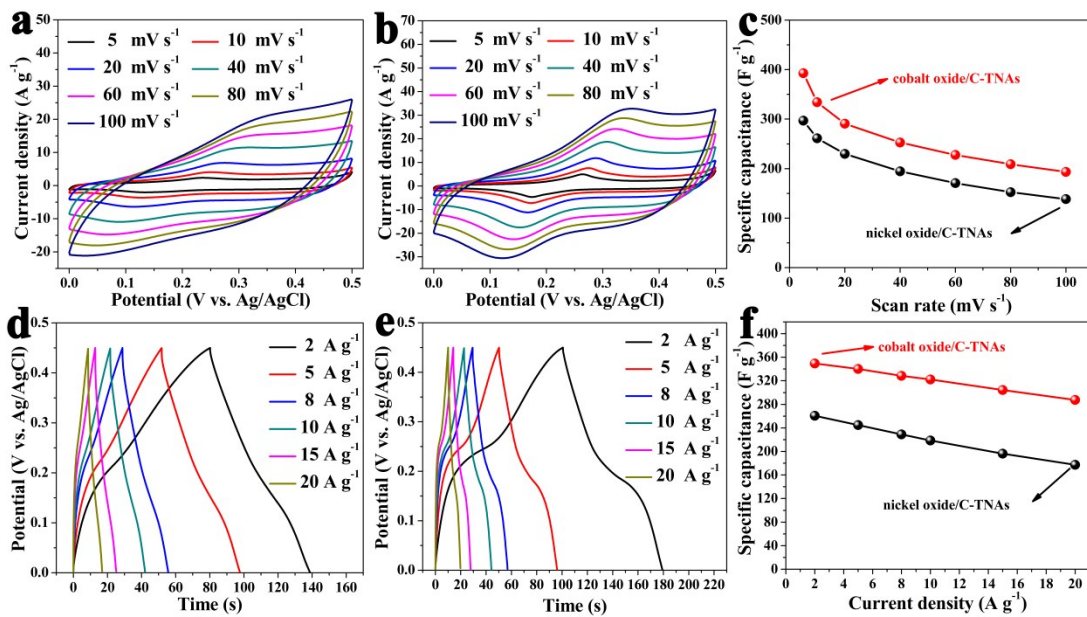


Fig. S9. CV curves of a) nickel oxide/C-TNAs; b) cobalt oxide/C-TNAs; c) specific capacitance plots with increasing scan rates; CD curves of c) nickel oxide/C-TNAs; d) cobalt oxide/C-TNAs; e) specific capacitance plots with increasing current densities.

Table S4 Comparison of supercapacitors based on TNAs-based and nickel cobalt oxides-based electrodes

Electrode materials	Synthesis approach	Electrolyte	Specific capacitance [F g ⁻¹]	Ref.
MnO ₂ /H-TiO ₂	Electrodeposition	0.5 M Na ₂ SO ₄	912 (10 mV s ⁻¹)	[3]
PANI/H-TiO ₂ NTs	Polymerization	1 M HCl	999 (0.6 A g ⁻¹)	[4]
MnO ₂ -TiO ₂ /C	Electrochemical deposition	1 M Na ₂ SO ₄	580 (2.6 A g ⁻¹)	[5]
CNF@NiCo ₂ O ₄	Solution method	2 M KOH	902 (2 A g ⁻¹)	[6]
	Thermal treatment			
NiCo ₂ O ₄ arrays	Hydrothermal	2 M KOH	1089 (2 A g ⁻¹)	[7]
porous NiCo ₂ O ₄	Hydrothermal	2 M KOH	832 (1 mV s ⁻¹)	[8]
nickel cobalt oxides /C-TNAs	CBD	2 M KOH	934.9 (2 A g ⁻¹)	This work

References

- 1 C. Shang, S. Dong, S. Wang, D. Xiao, P. Han, X. Wang, L. Gu and G. Cui, *ACS Nano*, 2013, 7, 5430–5436.
- 2 U. M. Patil, M. S. Nam, J. S. Sohn, S. B. Kulkarni, R. Shin, S. Kang, S. Lee, J. H. Kim and S. C. Jun, *J. Mater. Chem. A*, 2014, 2, 19075–19083.
- 3 X. H. Lu, G. M. Wang, T. Zhai, M. H. Yu, J. Y. Gan, Y. X. Tong and Y. Li, *Nano Lett.*, 2012, 12, 1690.
- 4 J. q. Chen, Z. B. Xia, H. Li, Q. Li and Y. J. Zhang, *Electrochim. Acta*, 2015, **166**, 174.
- 5 B. Gao, X. X. Li, Y. W. Ma, Y. Cao, Z. Y. Hu, X. M. Zhang, J. J. Fu, K. F. Huo and P. K. Chu, *Thin Solid Films*, 2015, 584, 61.
- 6 G. Q. Zhang and X. W. Lou, *Sci. Rep.*, 2013, **3**, 1470.
- 7 X.Y. Liu, Y.Q. Zhang, X.H. Xia, S.J. Shi, Y. Lu, X.L. Wang, C.D. Gu and J.P. Tu, *J. Power Sources*, 2013, **239**, 157.
- 8 T. Zhu, E. R. Koo and G. W. Ho, *RSC Adv.*, 2015, **5**, 1697.